Protoplasma (2015) 252:3–20
DOI 10.1007/s00709-014-0661-9

REVIEW ARTICLE

# Anatomical and ultrastructural adaptations of seagrass leaves: an evaluation of the southern Atlantic groups

**Chirle Ferreira · Paulo A. Horta · Gabriela M. Almeida · Carmen S. Zitta · Eliana de M. Oliveira · Marietou B. Y. B. Gueye · Ana C. Rodrigues**

Received: 12 December 2013 / Accepted: 21 May 2014 / Published online: 4 June 2014


**Abstract** Seagrasses, which form an integral part of the worldwide coastal habitat, are considered highly relevant from an ecological point of view. Due to the scarcity of anatomical information, the present study analyzed the morphoanatomy, histochemistry, and ultrastructure of *Halophila decipiens*, *Halodule wrightii*, and *Ruppia maritima* leaves, discussing their adaptations to the marine environments observed throughout the southwestern tropical and subtropical Atlantic coast. The leaves of these three species feature a uniseriate epidermis with the presence of chloroplasts in large quantities and absence of stomata. The vascular system consists of a central vascular bundle with sieve tube elements of the phloem and protoxylem lacunae, as well as small vascular bundles near the leaf margins. The leaves of *H. decipiens* possess trichomes, but no mesophyll in the leaf margins. The mesophyll of *H. wrightii* and *R. maritima* is homogeneous with chlorenchyma cells and air lacunae scattered throughout the leaf. The histochemistry analysis revealed the absence of amyloplasts and the presence of proteins in the outer periclinal walls of ordinary epidermal cells of the three species. It was also possible to detect the presence of idioblasts containing phenolic compounds in *H. decipiens* and *R. maritima*. The ultrastructural analysis of the three species revealed many elliptical chloroplasts, with organized thylakoids, expansion of the epidermal cell wall into the cytoplasm, and a thin cuticle. Hydropoten were also observed in the three specimens. The results show that the species analyzed have important adaptations which enable their survival in the marine environment.

**Keywords** Hydropoten · Phenolics contents · *Halophila* · *Halodule* · *Ruppia*

Handling Editor: Néstor Carrillo

C. Ferreira
Post-graduate Program in Plant Biology, Department of Botany, Federal University of Santa Catarina, 88040-900 Florianopolis, SC, Brazil

P. A. Horta · M. B. Y. B. Gueye · A. C. Rodrigues (✉)
Department of Botany, Federal University of Santa Catarina, 88040-900 Florianopolis, SC, Brazil
e-mail: anclaro@ccb.ufsc.br

G. M. Almeida
Graduate Biology Science, Federal University of Santa Catarina, 88040-900 Florianopolis, SC, Brazil

C. S. Zitta
Post-graduate Program in Cell Biology, Department of Cell Biology, Embryology and Genetics, Federal University of Santa Catarina, 88040-900 Florianopolis, SC, Brazil

E. de M. Oliveira
Central Laboratory of Electron Microscopy, Federal University of Santa Catarina, 88040-900 Florianopolis, SC, Brazil

## Introduction

Among the flowering plants, fewer than 60 described species can survive completely submerged in saltwater. These plants are commonly known as seagrasses (Oliveira et al. 1999; Hemminga and Duarte 2000). These marine plants have their origins in the Cretaceous period (den Hartog 1970; McCoy and Heck 1976; Waycott 2000) based on at least three independent events, as demonstrated by phylogenetic studies based on molecular data (Les et al. 1997). Nowadays, these groups are classified within the subclass Alismatidae (Monocotyledonae), distributed in the families Hydrocharitaceae, Zosteraceae, Posidoniaceae, and Cymodoceaceae (Les and Tippery 2013).

These taxa are distributed worldwide, growing in shallow coastal waters, typically in muddy and sandy sediments (unconsolidated substrates), sometimes forming extensive submerged beds (Creed et al. 2004; Orth et al. 2006; Short et al. 2006). These subtidal areas present some particular environmental factors, which have, most likely, played a key

role throughout their evolutionary histories in the selection of specific anatomical and morphological adaptations. In a seminal work, Kuo and den Hartog (2006) describe these adaptations to the aquatic marine environment. Among the anatomical adaptations, the authors indicate that these marine plants present (1) leaves with thin cuticle, (2) small epidermal cells with thick wall, (3) concentrations of chloroplasts in epidermal cells, (4) absence of stomata, (5) a vast system of aerenchyma, and (6) reduced xylem. They also propose a set of characteristics that, when grouped together, can be taken as adaptations of seagrasses, such as strap-shaped leaves to resist the wave action, osmotic adjustment, and enzymatic conversion of $HCO_3^-$ seawater into $CO_2$, which occurs at the outer wall of epidermal cells.

The ecological importance of these groups is based on their role as a foundation species supplying food, substrate and shelter for many aquatic organisms (Short and Neckles 1999; Gullström et al. 2002), as a blue carbon species (Copertino 2011), and as protection for the coastline (Fonseca and Fisher 1986; Hemminga and Duarte 2000). As such, many studies have addressed seagrass taxonomy and ecology. However, the morphoanatomical adaptative strategies developed by these marine plants related to submersion, salinity, and irradiance availability are poorly addressed (Larkum et al. 2006). Therefore, the aim of this study is to complete this gap by describing the morphoanatomy, histochemistry, and ultrastructure features of the leaves of Brazilian species of seagrasses, highlighting adaptive answers found by these species in these complex and heterogeneous marine environments.

## Materials and methods

### Plant material

For this study, the leaf blades used were of individuals of the species *Halophila decipiens* Ostenf. (Hydrocharitaceae), *Halodule wrightii* Asch. (Cymodoceaceae), and *Ruppia maritima* L. (Cymodoceaceae), all of which occur in Brazil, the most abundant and important representative of the group along the southwestern tropical and subtropical Atlantic coast (Oliveira et al. 1999). The species were collected from different locations (Table 1); two sampling points were selected at each collection point where an average of 10 individuals of each species was collected.

### Light microscopy and histochemical tests

The material was fragmented into smaller pieces with the aid of a razor blade to analyze the mid region, including the fully expanded leaf margins. Subsequently, the material was fixed with 2.5 % glutaraldehyde in 0.1 M sodium phosphate buffer (pH 7.2), for at least 3 h. For prepared permanent slides, the samples were dehydrated in increasing series of aqueous ethanolic solutions and then infiltrated by historesin (Leica Historesin, Heidelberg, Germany). Cross sections of 5 μm was submitted to various histochemical tests: toluidine blue O (TB-O) for analysis of general anatomy and acidic polysaccharides by metachromatic reaction (Gordon and McCandless 1973); Coomassie Brilliant Blue (CBB) for total proteins (Gahan 1984), periodic acid-Schiff (PAS) for neutral polysaccharides (Gahan 1984), and ferric chloride for phenolic compounds (Johansen 1940).

The material was analyzed and photographed with a light microscope (Olympus, model BX41) equipped with camera image capture digital color with 3.3 Mpx coupled Q-imaging and the image capture program Q-Capture Pro 5.1 (Multiuser Laboratory of Studies in Biology II (LAMEB II), Centre of the Biological Sciences of the Federal University of Santa Catarina, Brazil).

### Transmission electron microscopy

Observations of transmission electron microscopy (TEM) were performed on samples fixed overnight with 2.5 %

**Table 1** List of the species collected, collection sites, and registration number of the exsiccates of the specimens in the herbarium

| Species | Collection sites | Geographic coordinates | [a]Number of the herbarium |
|---|---|---|---|
| *Halophila decipiens* Ostenfeld | Abrolhos Archipelago (southern Bahia) | 17° 20′ S–18° 10′ S and 38° 35′ W–39° 20′ W | FLOR0029186 |
| | Saco da Ribeira (Ubatuba, SP) | 23° 22′ S and 44° 48′ W | FLOR0051104 |
| *Halodule wrightii* Ascherson | Itamaracá Island (Recife, PE) | 7° 45′ S and 34° 51′ W | FLOR0051106 |
| | Abrolhos Archipelago (southern Bahia) | 17° 20′ S–18° 10′ S and 38° 35′ W–39° 20′ W | FLOR0038224 |
| | Saco da Ribeira (Ubatuba, SP) | 23° 22′ S and 44° 48′ W | FLOR0051105 |
| | Channel of the Lagoa da Conceição (Florianópolis, SC) | 27° 34′ 47″ S and 48° 25′ 47″ W | FLOR0051113 |
| *Ruppia maritima* Linnaeus | Lagoa de Acarai (South San Francisco, SC) | 26° 17′ 25″ S and 48° 32′ 50″ W | FLOR0051111 |
| | Channel of the Lagoa da Conceição (Florianópolis, SC) | 27° 34′ 47″ S and 48° 25′ 47″ W | FLOR0051115 |
| | Lagoa da Conceição (Florianópolis, SC) | 27° 36′ 22″ S and 48° 27′ 47″ W | FLOR0051118 |

[a] Specimens of the taxon studied in different collection points were deposited in Herbarium FLOR (UFSC, Florianópolis, SC)

gluteraldehyde in 0.1 M sodium phosphate buffer (pH 7.2). The material was postfixed with 1 % osmium tetroxide (OsO4) in 0.1 M sodium phosphate buffer, for 4 h, dehydrated in a graded acetone series, and infiltrated with Spurr's resin. Ultrathin sections were made with a diamond blade using an ultramicrotome (Leica, model EMUC7, Germany), followed by staining with 1 % uranyl acetate and 1 % lead citrate. The samples were examined under TEM JEM 1011 (JEOL Ltd., Tokio, Japan, at 80 kV), using the Central Laboratory of Electron Microscopy of UFSC, Brazil, core facility.

## Results

### Anatomy and histochemistry

#### *Halophila decipiens*

The leaf blade of *H. decipiens*, in transverse sections, has a uniseriate epidermis with stomata absent (Fig. 1a–f). The epidermal cells on both sides are rectangular, except in the region of the midrib and lateral vascular bundles, which are rounded (Fig. 1a–f). In parademic view, on both sides of the leaf blade, the epidermal cells have polygonal shapes of similar size, with straight anticlinal cell walls, gently undulating, with a large presence of chloroplasts (Fig. 1g). Unicellular trichomes can be present in the leaf margin (Fig. 1g), as observed in specimens collected from Bahia and São Paulo. In the São Paulo specimens, unicellular trichomes were also found in the leaf blades, both adaxial and abaxial sides (Fig. 1e, f, h).

The leaves of *H. decipiens* have no mesophyll (Fig. 1a, c). The vascular system is formed by vascular bundles of larger size located in the midrib (Fig. 1b) and two reduced peripheral bundles located at the leaf margins (Fig. 1a, c). In the central region, the chlorenchyma is observed with two small aerenchyma lacunae (Fig. 1b, d), the midrib with collateral vascular bundle formed by protoxylem lacunae of small diameter, and a few sieve tube elements (Fig. 1b). The presence of idioblasts was not observed in the leaf blade of *H. decipiens*.

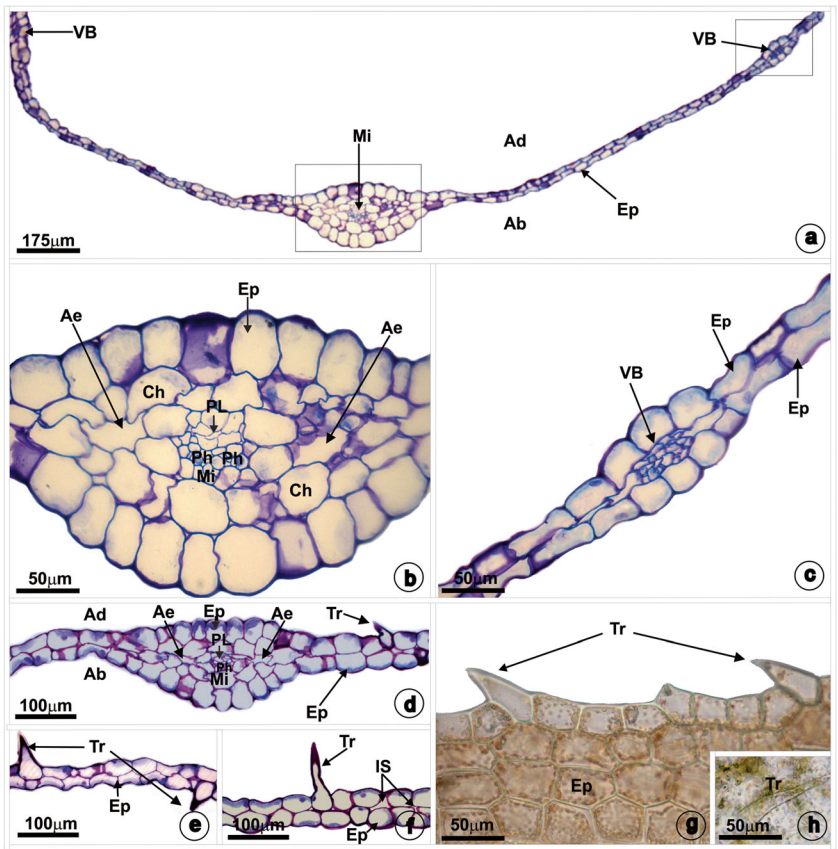


**Fig. 1** Photomicrographs of transverse sections (**a**–**f**) and parademic sections (**g**, **h**) of the leaf blade of *Halophila decipiens* Ostenf. Staining: toluidine blue O (TB-O) (**a**–**f**) and no staining (**g**, **h**). **a**–**c** Abrolhos Archipelago (BA). **d**–**h** Saco da Ribeira (SP). **a** General aspect of the leaf blade. **b** Detail of the central region showing the uniseriate epidermis, the chlorenchyma, and the midrib. **c** Detail of leaf margins showing the vascular bundle and the absence of mesophyll. **d** Detail of the central region. **e**, **f** Detail of the region of the leaf margins showing trichomes on both adaxial and abaxial sides and the intercellular spaces (**f**). **g** Parademic view of the adaxial side showing epidermal cells with chloroplasts and presence of trichome on the leaf surface. **h** Detail of an epidermal trichome in parademic view. *Ab* abaxial side, *Ad* adaxial side, *Ae* aerenchyma lacunae, *Ch* chlorenchyma, *Ep* epidermis, *IS* intercellular space, *PL* protoxylem lacunae, *Mi* midrib, *Ph* phloem, *VB* vascular bundle, *Tr* trichome

The analysis with PAS revealed the absence of amyloplasts in the leaf blade (Fig. 2a–c). The outer periclinal walls of ordinary epidermal cells showed a positive reaction to PAS (Fig. 2a, b, arrow) and CBB (Fig. 2d, black arrow), indicating the presence of neutral polysaccharides and proteins, respectively. The walls of trichomes also showed a positive PAS reaction (Fig. 2c), as well as the outer cytoplasm, which also reacted with CBB (Fig. 2e).

Results also highlight a positive CBB reaction in the periphery of the cytoplasm of ordinary epidermal cells, revealing the presence of a large amount of cytoplasmic organelles in this region, probably chloroplasts (Fig. 2d, f).

*Halodule wrightii*

The leaf blade of *H. wrightii*, in transverse sections, presents a uniseriate epidermis (Fig. 3a–f), whose cells have a rounded shape (Fig. 3a–f), thick outer periclinal cell walls (Fig. 3f, arrow). The mesophyll is homogeneous (Fig. 3a–d), consisting of relatively large, rounded parenchymal cells, with thin walls, which delimit larger or smaller intercellular spaces, characterizing aerenchyma (Fig. 3a–g). The vascular system is constituted by three vascular bundles, a central bundle with larger diameter and two smaller bundles located near the leaf margins (Fig. 3a–d). The vascular bundle of larger size is the collateral type, formed by a lacuna of protoxylem, a few sieve tube elements, and parenchyma cells surrounded by two sheaths of parenchymatous cells (Fig. 3f, g).

In paradermic view on both sides, the epidermal cells have a rectangular shape, with straight and thick anticlinal cell walls, with a large presence of chloroplasts (Fig. 3h), not revealing the presence of trichomes or stomata (Fig. 3h, i).

Idioblasts occur in large amounts in the chlorenchyma near the epidermis (Fig. 4a, b) and in the epidermis (Fig. 4c, d). The

**Fig. 3** Photomicrographs of transverse sections (**a**–**g**) and paradermic sections (**h**, **i**) of the leaf of *Halodule wrightii* Aschers. Staining: toluidine blue O (TB-O) (**a**–**g**) and no staining (**h**–**i**). **a** Itamaracá Island (PE). **b** Abrolhos Archipelago (BA). **c** Saco da Ribeira (SP). **d** Channel of the Lagoa da Conceição (SC-3). **a**–**d** General aspect of the leaf showing uniseriate epidermis, mesophyll with chlorenchyma, idioblasts, midrib, reduced vascular bundles in the leaf margins, and a network of aerenchyma lacunae. **e** Leaf margins evidencing epidermal cytoplasm with positive reaction to TB-O, revealing concentration of acidic polysaccharides, presence of idioblasts in mesophyll, and vascular bundles with sieve tube elements and absence of the protoxylem lacunae. **f** Detail of the air lacunae of the mesophyll and epidermis with thick outer periclinal cell walls (*arrow*). **g** Detail of the central region of the leaf showing the parenchymatic sheath (two layers) and the central vascular bundle with protoxylem lacunae and phloem. **h** Paradermic view of the adaxial side showing epidermal cells with chloroplasts (*arrow*). **i** Detail of the leaf margins. *Ab* abaxial side, *Ad* adaxial side, *Ae* aerenchyma lacunae, *Ch* chlorenchyma, *Ep* epidermis, *Id* idioblast, *Mi* midrib, *ph* phloem, *VB* vascular bundle, *PL* protoxylem lacunae, *Sh* sheath, *ST* sieve tube

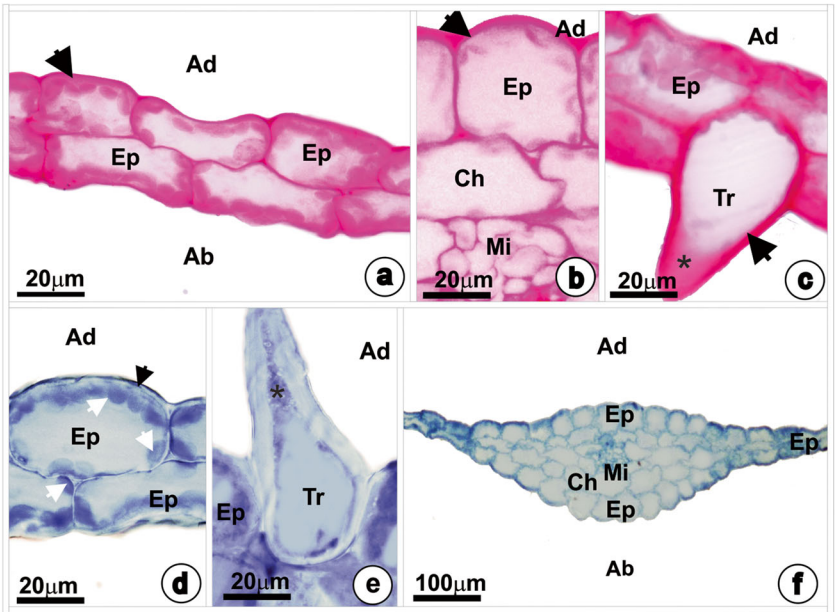


**Fig. 2** Photomicrographs of transverse sections of the leaf blade of *Halophila decipiens* Ostenf. Treated with periodic acid-Schiff (PAS) (**a**–**c**) and Coomassie Brilliant Blue (CBB) (**d**–**f**). **a**–**b** Detail of the epidermal cells of the leaf margins (**a**) and midrib (**b**) showing positive reaction of cell walls to PAS (*black arrow*). **c** Detail of unicellular trichome showing positive reaction to PAS in the periphery of the cytoplasm (*asterisk*) and the cell wall. **d** Details of foliar leaf margin epidermal cells with positive reaction to CBB in the periphery of the cytoplasm (*white arrow*) and in the outermost periclinal walls (*black arrow*), evidencing the presence of protein in these regions. **e** Unicellular trichome showing positive reaction to CBB in the cytoplasm, being more intense in the peripheral region, especially near the outer region (*asterisk*). **f** Midrib showing positive reaction to CBB in the periphery of the cytoplasm. *Ch* chlorenchyma, *Ep* epidermis, *Ab* abaxial side, *Ad* adaxial side, *Mi* midrib, *Tr* trichome

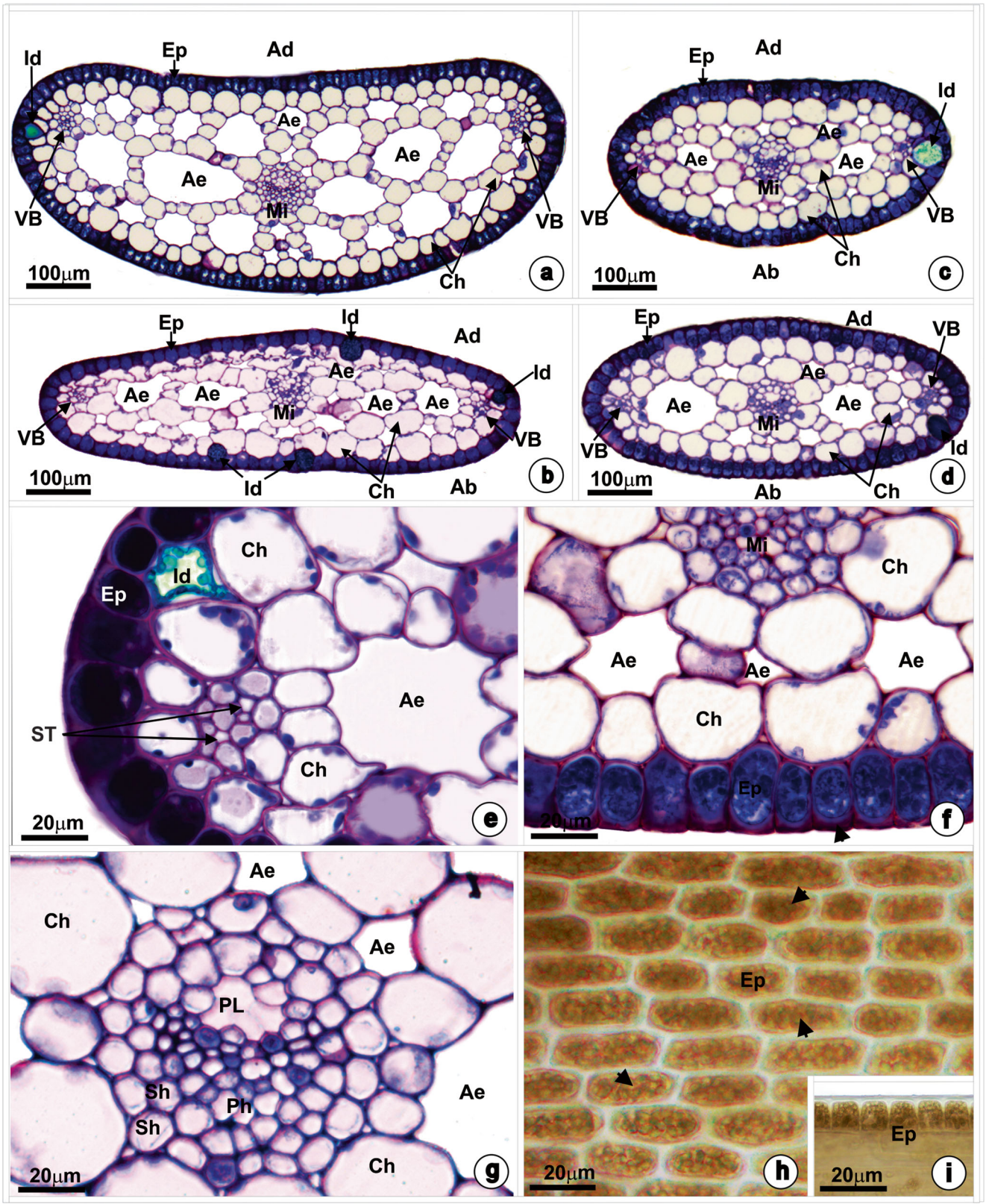


content of idioblasts showed differential reaction to TB-O with a metachromatic reaction manifesting a greenish blue color (Fig. 4a–d) and a positive reaction to ferric chloride, indicating the presence of phenolic compounds. Figure 4

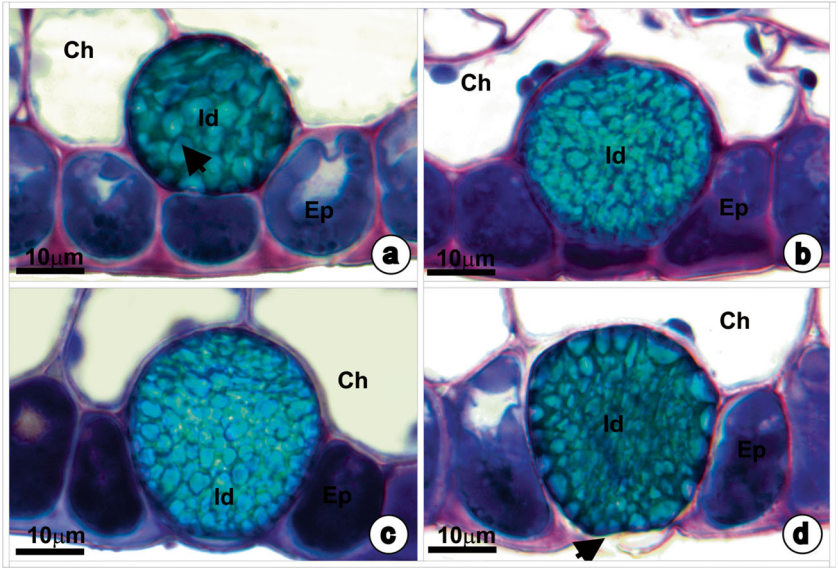


**Fig. 4** Photomicrographs of transverse sections of the leaf blade of *Halodule wrightii* Aschers., evidencing the idioblasts. Staining: toluidine blue O (TB-O). **a**–**d** Sequence follows idioblasts of the mesophyll (**a**, **b**) to the epidermis (**c**, **d**) with epidermal cell wall rupture (*black arrow*) (**d**). *Ch* chlorenchyma, *Ep* epidermis, *Id* idioblast

shows the sequence of idioblasts coming out of the mesophyll toward the outside where a ruptured outer periclinal cell wall releases the contents outwards (Fig. 4d, arrow).

From both sides of the epidermal cell walls, mesophyll and the central vascular bundle reacted positively to PAS (Fig. 5a–c), as well as TB-O (Fig. 3e, f), confirming the concentration of both neutral and acidic polysaccharides in these regions. PAS revealed the absence of amyloplasts in the leaf blade (Fig. 5a–c). Attention is called to the positive reaction to CBB in the outermost layer of periclinal walls of the epidermis (Fig. 5a, b). The content of epidermal cells reacted strongly to TB-O (Fig. 3e, f), PAS (Fig. 5a, b), and CBB (Fig. 5f, g), showing high concentrations of acidic polysaccharides and neutral proteins in this region. The mesophyll did not manifest this reaction. The idioblasts only reacted to TB-O, not PAS (Fig. 5d, e) or CBB (Fig. 5i). CBB also revealed the presence of a few organelles in mesophyll cells (Fig. 5f–i), being found in larger amount in the central vascular bundle (Fig. 5h).

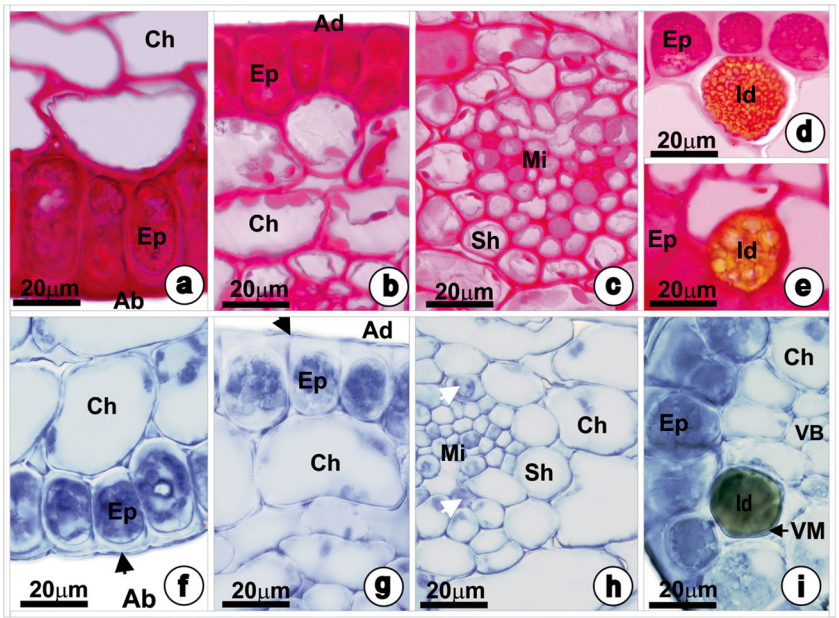


**Fig. 5** Photomicrographs of transverse sections of the leaf blade of *Halodule wrightii* Aschers. treated with periodic acid-Schiff (PAS) (**a**–**e**) and Coomassie Brilliant Blue (CBB) (**f**–**i**). **a**, **b** Detail of the abaxial (**a**) and adaxial (**b**) epidermis with cell wall and cytoplasm reacting positively to PAS, revealing concentration of neutral polysaccharides. **c** Detail of the central region. **d**, **e** Highlight of idioblasts with negative reaction to PAS. **f**, **g** Detail of the abaxial (**a**) and adaxial (**b**) epidermis and the chlorenchyma cells with positive reaction to CBB in the cytoplasm, with a more intense reaction in the epidermis, and in the outermost periclinal walls of the epidermis (*arrow*). **h** Midrib with positive reaction to CBB in the organelles (*white arrows*). **i** Highlight of an idioblast showing the vacuolar content with negative reaction to CBB. *Ab* abaxial side, *Ad* adaxial side, *Ch* chlorenchyma, *Ep* epidermis, *Id* idioblast, *Mi* midrib, *MV* vacuole membrane, *Sh* sheath, *VB* vascular bundle

*Ruppia maritima*

The leaf blade of *R. maritima*, in transverse cross sections, showed uniseriate epidermal cells with a rounded shape and thin walls (Fig. 6a–f), which, like other cell walls of the mesophyll, showed reaction to TB-O by a uniform purple coloration (Fig. 6d–g).

On both sides, the paradermic view revealed epidermal cells with a rectangular cubical shape of slightly different sizes. Stomata are absent, but chloroplasts show a significant presence (Fig. 6h). Unicellular or multicellular trichomes with the presence of chloroplasts mainly occur on the margins of the leaf blade near the apex (Fig. 6i).

The mesophyll is homogeneous and consists of rounded cells with thin walls, which delimit two conspicuous cavities of the aerenchyma, one on each side of the midrib (Fig. 6a–c). The vascular system is composed of three vascular bundles, a larger vascular bundle located in the midrib and two smaller vascular bundles located near the leaf margins (a–c). Typically, the smaller bundles are not found on the entire leaf blade (Fig. 6d) until they reach the middle region, never reaching the leaf apex. These bundles only have a few sieve tube elements, on average two, and a sheath of parenchyma cells, while the presence of protoxylem lacunae is not observed (Fig. 6e). The larger vascular bundle is the collateral type formed by protoxylem lacunae, a few sieve tube elements and parenchyma

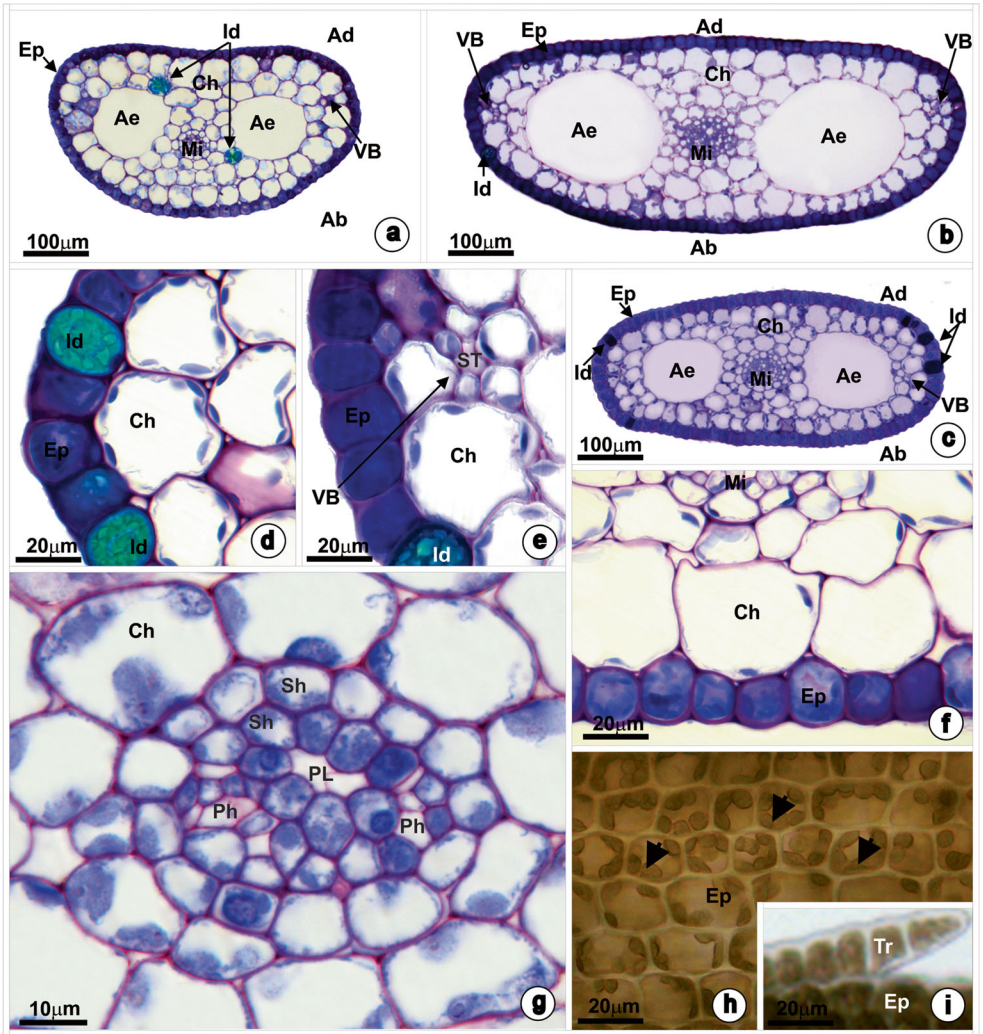


**Fig. 6** Photomicrographs of transverse sections (**a**–**f**) and paradermic sections (**g**, **h**) of the leaf blade of *Ruppia maritma* L. Staining: toluidine blue O (TB-O) (**f**) and no staining (**g**, **h**). **a** Lagoa de Acarai (SC). **b** Lagoa da Conceição (SC). **c** Channel of the Lagoa da Conceição (SC). **a**–**c** General aspect of the leaf blade. **d**, **e** Details of the leaf margins. Leaf margins without vascular bundles; idioblasts are observed in the epidermis with metachromatic reaction to TB-O (**d**); leaf margins with vascular bundles with sieve tube element and absence of the protoxylem lacunae. **f** Detail of epidermis with positive reaction to TB-O in the cytoplasm, showing great concentration of acidic polysaccharides and absence of reaction in the chlorenchyma. **g** Detail of the central vascular bundle. **h** Paradermic view of the adaxial side showing the epidermal cells with straight and thickened walls and presence of chloroplasts (*arrows*). **i** Detail of the leaf margins showing the presence of multicellular trichomes. *Ab* abaxial side, *Ad* adaxial side, *Ae* aerenchyma lacunae, *Ch* chlorenchyma, *Ep* epidermis, *Id* idioblast, *Mi* midrib, *Ph* phloem, *PL* protoxylem lacuna, *Sh* sheath, *ST* sieve tube, *Tr* trichome, *VB* vascular bundle

cells, being surrounded by two sheaths of parenchyma cells (Fig. 6g). In *R. maritima* leaf blades, idioblasts were observed in the central vascular bundle (Fig. 7a) in the mesophyll cells (Fig. 7b) and in the epidermis (Fig. 7c). Their contents showed differential reaction to TB-O, with a metachromatic reaction expressing a greenish blue color (Fig. 7a–d) and a positive reaction to ferric chloride, indicating the presence of phenolic compounds. Figure 7c shows secretion of idioblast content outside the epidermis. Details of the ruptured outer periclinal cell wall are seen in Fig. 7d (arrow), and an idioblast without content is visible in Fig. 7e.

On both sides of the epidermal cells walls, the mesophyll and central vascular bundle showed a positive reaction to PAS (Fig. 8a, b), as well as TB-O, showing a concentration of both neutral and acidic polysaccharides in these regions. The outer periclinal walls of the epidermal cells showed a positive reaction to CBB in their outermost portion (Fig. 8f, g). The content of epidermal cells reacted strongly to TB-O (Fig. 6d–f), PAS (Fig. 8a, b), and CBB (Fig. 8f, g). The mesophyll showed no reaction. The idioblasts reacted only to TB-O (Fig. 7a–e), not PAS (Fig. 8d, e) or CBB (Fig. 8i, j). CBB also revealed the presence of a few cytoplasmic organelles in the mesophyll (Fig. 8f, g), being found in larger amounts in the central vascular bundle (Fig. 8h).

## Ultrastructure of the leaf blade

### *Halophila decipiens*

Transmission electron micrographs of transverse sections of the leaf blade of *H. decipiens* showed epidermal cells with extensive presence of chloroplasts in the peripheral region (Fig. 9a), mitochondria next to chloroplasts (Fig. 9a–c), and a large central nucleus (Fig. 9a). The outer periclinal wall of epidermal cells is thicker compared to the inner periclinal walls where it is possible to distinguish a more electron-dense layer (Fig. 9b), which appears to correspond to protein deposition observed under light microscopy (Fig. 2d). External to this wall is a thin layer which is even more electron-dense (Fig. 9b). Expansions of wall cells are visible in epidermal cells (Fig. 9b, arrow). Next to the expansions are found several mitochondria. These expansions were not found in the mesophyll cells, even those in direct contact with the epidermis.

The chloroplasts of both epidermal (Fig. 9a, c, d) and mesophyll cells (Fig. 10a, b) have an elliptical shape arranged with organized thylakoids, many plastoglobules, no starch grains, and similar amounts of thylakoids by granum, i.e., by stacks of thylakoid disks. However, in the epidermal cells, the chloroplasts were observed to be slightly larger and more abundant.

The mesophyll cells have thin cell walls and large vacuoles located centrally, leaving the cytoplasm restricted to the periphery, where chloroplasts and other organelles are distributed (Fig. 10a). Mitochondria are also located right next to the chloroplasts.

The sieve tube elements of the central vascular bundle have thin cell walls and large lumen (Fig. 10c, d). The sieve tube elements also contain mitochondria (Fig. 10c) and P-type plastids with cuneiform protein inclusions (Fig. 10d). Parenchyma cells in the bundle sheath may be observed in Fig. 10 (c, d), as well as a companion cell (Fig. 10d).

### *Halodule wrightii*

Transmission electron micrographs of transverse sections of the leaf blade of *H. wrightii* revealed epidermal cells with extensive presence of chloroplasts distributed throughout the

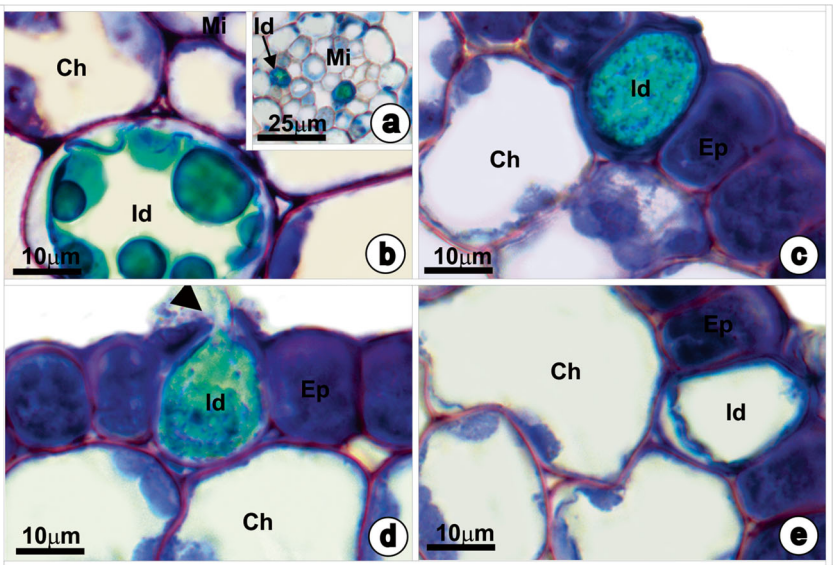


**Fig. 7** Photomicrographs of transverse sections of the leaf blade of *Ruppia maritima* L., evidencing the idioblasts. Staining: toluidine blue O (TB-O). **a** Idioblast in the midrib. **b** Idioblast in the mesophyll near the midrib. **c** Idioblast in the epidermis. **d** Periclinal outer wall cell of the epidermal idioblast with rupture (*black arrow*). **e** Idioblast without vacuole content. *Ch* chlorenchyma, *Ep* epidermis, *Id* idioblast, *Mi* midrib

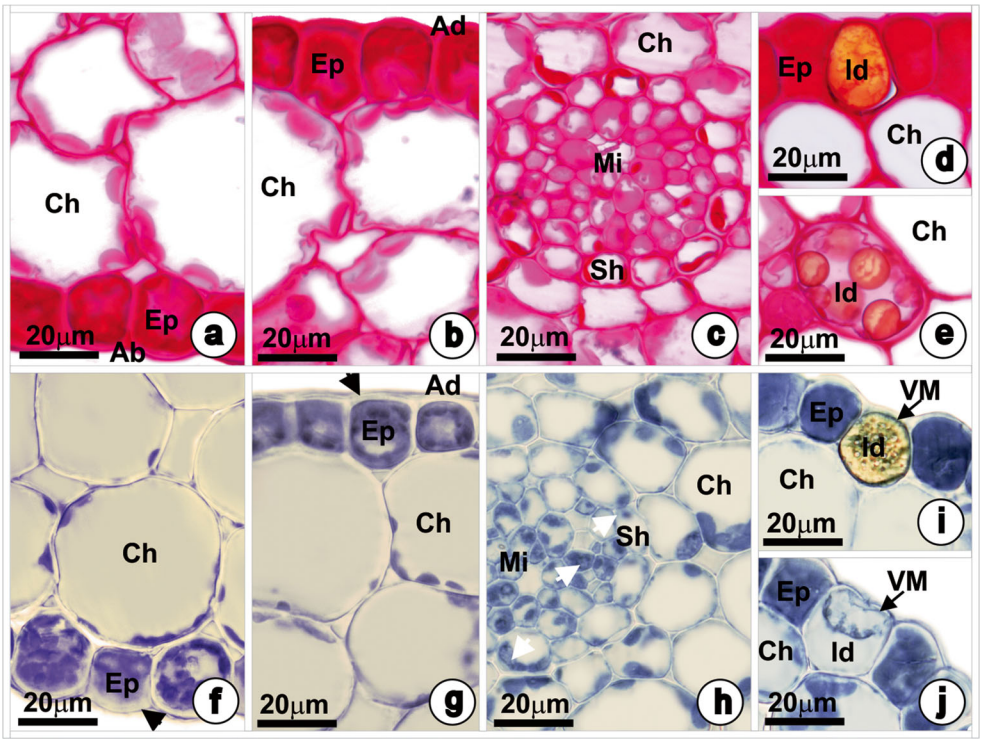


**Fig. 8** Photomicrographs of transverse sections of the leaf blade of *Ruppia maritima* L. treated with periodic acid-Schiff (PAS) (**a**–**e**) and Coomassie Brilliant Blue (CBB) (**f**–**j**). **a**, **b** Detail of the abaxial (**a**) and adaxial (**b**) epidermis with cell wall and cytoplasm reacting positively to PAS, revealing concentration of neutral polysaccharides. **c** Detail of the central region. **d**, **e** Highlight of idioblasts with negative reaction to PAS. **f**, **g** Detail of the abaxial (**a**) and adaxial (**b**) epidermis and of the chlorenchyma cells with positive reaction to CBB in the cytoplasm, with a more intense reaction in the epidermis and in the outermost periclinal walls of the epidermis (**g**, *arrow*). **h** Midrib with positive reaction to CBB in the organelles (*white arrows*). **i** Highlight of an idioblast, showing vacuolar content with negative reaction to CBB. **j** Idioblast without differential content in the vacuole. *Ab* abaxial side, *Ad* adaxial side, *Ch* chlorenchyma, *Ep* epidermis, *Id* idioblast, *Mi* midrib, *MV* vacuole membrane, *Sh* sheath

cytoplasm, with higher concentration in the peripheral region, a central vacuole, and a small nucleus located next to the vacuole (Fig. 11a). Many expansions are visible in the cell walls of the epidermal cells (Fig. 11b, arrow). These expansions are found in anticlinal cell walls, but they sometimes also affect the external and internal periclinal walls. Expansions are found near the mitochondria (Fig. 11b). No expansions were found in the mesophyll cells, even those in direct contact with the epidermis.

The outer periclinal cell wall of the epidermis cell is very thick compared to the inner periclinal wall, showing four distinct zones: a thickened, nonelectron-dense layer can be observed from the inside to the outside, followed by another thickened, electron-dense layer, which appears to correspond to protein deposition observed in light microscopy (Fig. 5f, g), a third thin layer, even more electron-dense, and located externally, and an electron-transparent layer with presence of small cavities (Fig. 11c).

Another type of idioblast was present in the epidermis, but it could not be identified under light microscopy. These structures contain many mitochondria localized in the peripheral region of the cytoplasm next to the mesophyll, many vesicles localized in the peripheral region of the cytoplasm next to the outer periclinal wall, and many expansions of the cell walls, principally the outer periclinal walls, occupying a large part of cytoplasm (Fig. 11d). In this cell, the periclinal outer wall may be up to three times thicker than the other epidermal cells, and chloroplasts do not occur.

Chloroplasts of both epidermal (Fig. 12a, b) and mesophyll cells (Fig. 12c, d) have an elliptical shape with organized thylakoids arranged by granum, a large amount of plastoglobules and no starch grains. However, in the epidermal cells, the chloroplasts were observed to be slightly larger, having four times the volume of the mesophyll chloroplasts, and they were more abundant.

The mesophyll cells have thin cell walls, and the presence of a centrally located large vacuole restricted to the periphery of the cytoplasm in which chloroplasts and other organelles are distributed (Fig. 12c).

Sieve tube elements can be observed in the central vascular bundle. These have thickened cell walls of the nacreous type, small cell lumen and companion cells (Fig. 13a–c). On the inside of sieve tube elements, large P-type plastids are found with granular protein inclusions (Fig. 13b, d). Several cytoplasmic extensions of plasmodesma were observed between the cells of the vascular tissue, mostly between chlorenchyma

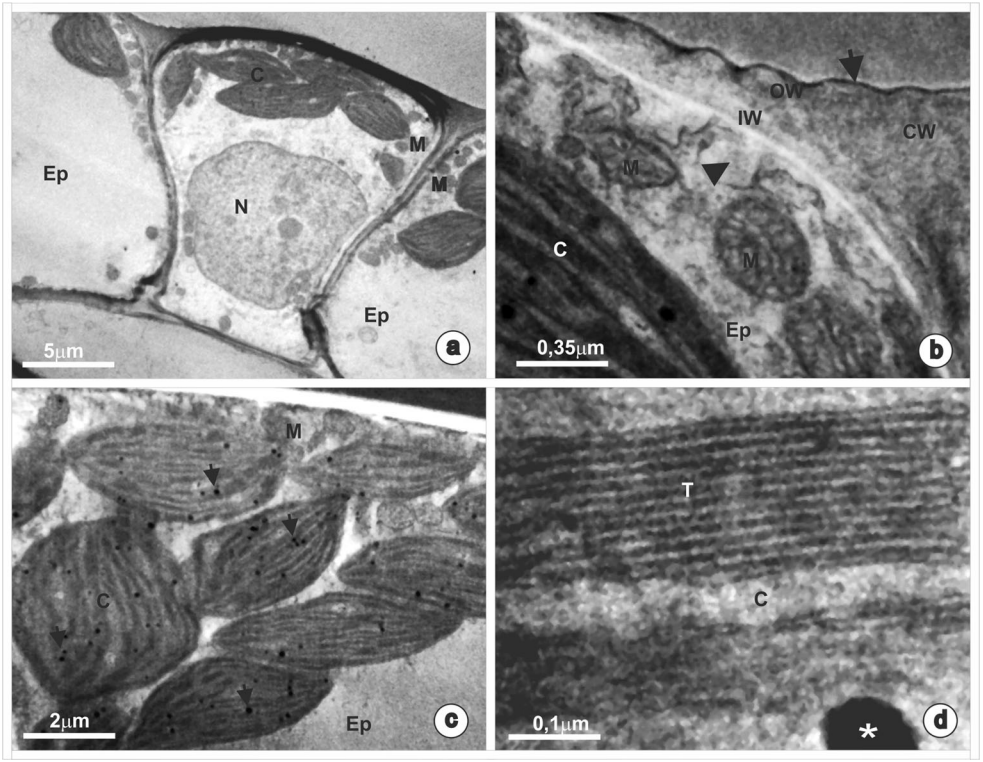


**Fig. 9** Transmission electron micrographs of transverse sections of the leaf epidermis of *Halophila decipiens* Ostenf. **a** Epidermal cells showing the presence of chloroplasts in the peripheral region, mitochondria, and large central nucleus. **b** Detail showing the outer periclinal cell walls with three distinct zones: a thin, nonelectron-dense layer (*IW*) can be observed from the inside to the outside, followed by a thicker, electron-dense layer (*OW*), and a third thin layer, even more electron-dense (*arrow*). Several expansions in the anticlinal cell walls are also visible (*arrowhead*). **c** Elliptical chloroplasts with many plastoglobules (*arrows*). **d** Details of the structure of a chloroplast with organized thylakoids and presence of plastoglobules (*asterisk*). *C* chloroplast, *Ch* chlorenchyma, *CW* cell wall, *Ep* epidermis, *IW* inner wall region, *M* mitochondria, *N* nucleus, *OW* outer wall region, *T* thylakoid

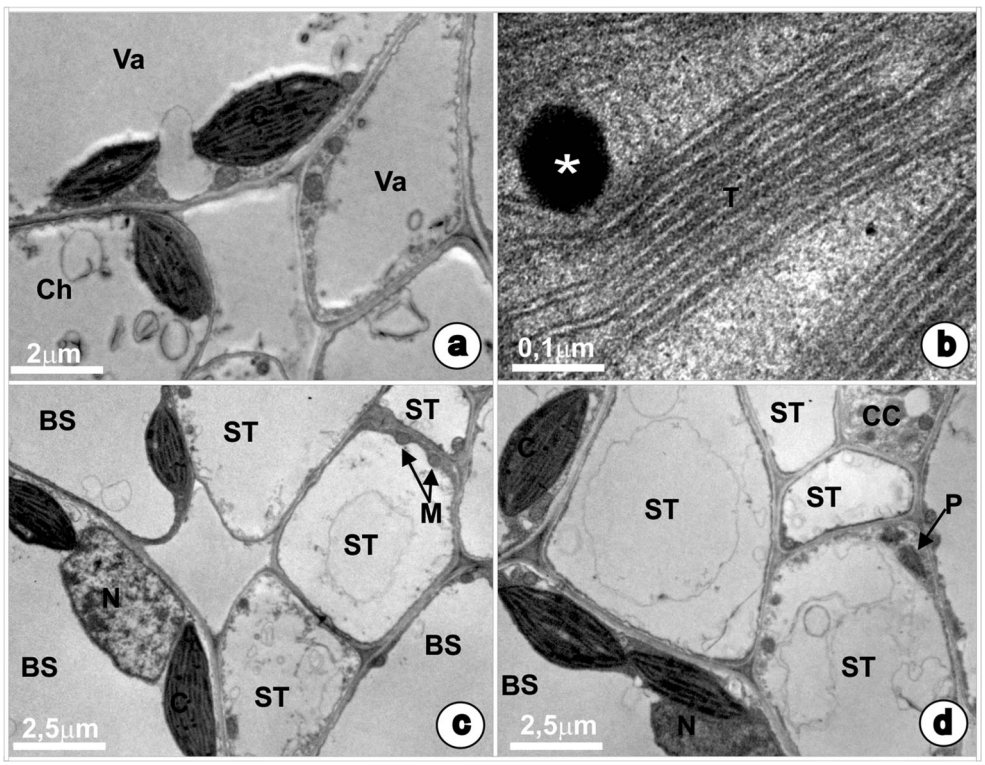


**Fig. 10** Transmission electron micrographs of transverse sections of the leaf blade midrib of *Halophila decipiens* Ostenf. **a** Detail of the mesophyll showing chlorenchyma cells with chloroplasts distributed in the periphery of the cytoplasm and large central vacuole. **b** Detail of the chloroplast structure with organized thylakoid and presence of plastoglobules (*asterisk*). **c**, **d** Central vascular bundle showing the sieve tube elements with thin cell walls and P-type plastids with cuneiform protein inclusions. *BS* bundle sheath, *C* chloroplast, *CC* companion cell, *Ch* chlorenchyma, *M* mitochondria, *N* nucleus, *P* plastid with protein inclusion, *ST* sieve tube, *T* thylakoids, *Va* vacuole

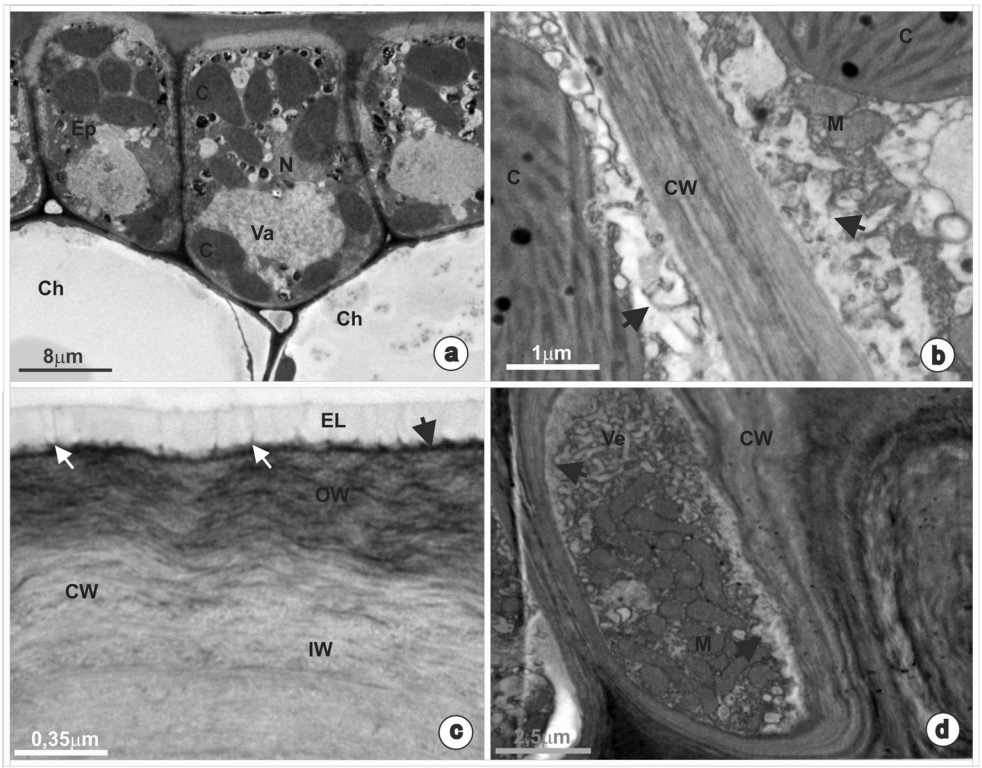


**Fig. 11** Transmission electron micrographs of transverse sections of the leaf epidermis of *Halodule wrightii* Aschers. **a** Epidermal cells showing the presence of chloroplasts scattered throughout the cytoplasm, nucleus, and vacuoles. **b** Detail of epidermal cell showing mitochondria near the chloroplast and the cell wall expansions (*arrows*). **c** Detail showing the outer periclinal cell walls with four distinct zones: a thickened, nonelectron-dense layer (*IW*) can be observed from the inside to the outside, followed by a thickened, electron-dense (*OW*) layer, a third thin layer (*black arrow*), even more electron-dense, and, finally, an electron-transparent layer with the presence of small cavities (*white arrows*). **d** Detail of an epidermal idioblast with an abundance of mitochondria, vesicles, and cell wall expansion. *C* chloroplast, *Ch* chlorenchyma, *Cu* cuticle, *CW* cell wall, *Ep* epidermis, *IW* inner wall region, *EL* electron-transparent layer, *M* mitochondria, *N* nucleus, *OW* outer wall region, *T* thylakoid, *Va* vacuole, *Ve* vesicles

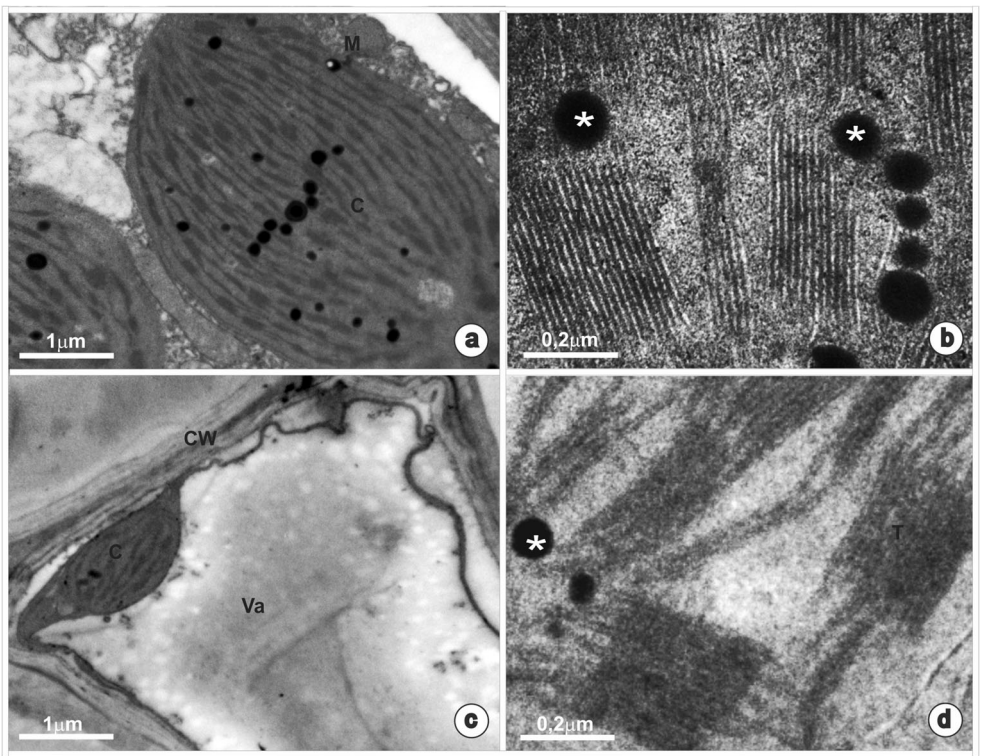


**Fig. 12** Transmission electron micrographs of transverse sections of the leaf blade of *Halodule wrightii* Aschers., evidencing chloroplasts of the epidermis (**a**, **b**) and mesophyll (**c**, **d**). **a**, **b** Detail of the structure of an epidermal chloroplast with organized thylakoid and presence of plastoglobules (*asterisk*). **c** Mesophyll cell showing chloroplast in the cytoplasm periphery and presence of a large central vacuole. **d** Detail of the structure of a chlorenchymatic chloroplast with organized thylakoid and presence of plastoglobules (*asterisk*). *C* chloroplast, *CW* cell wall, *M* mitochondria, *T* thylakoids, *Va* vacuole

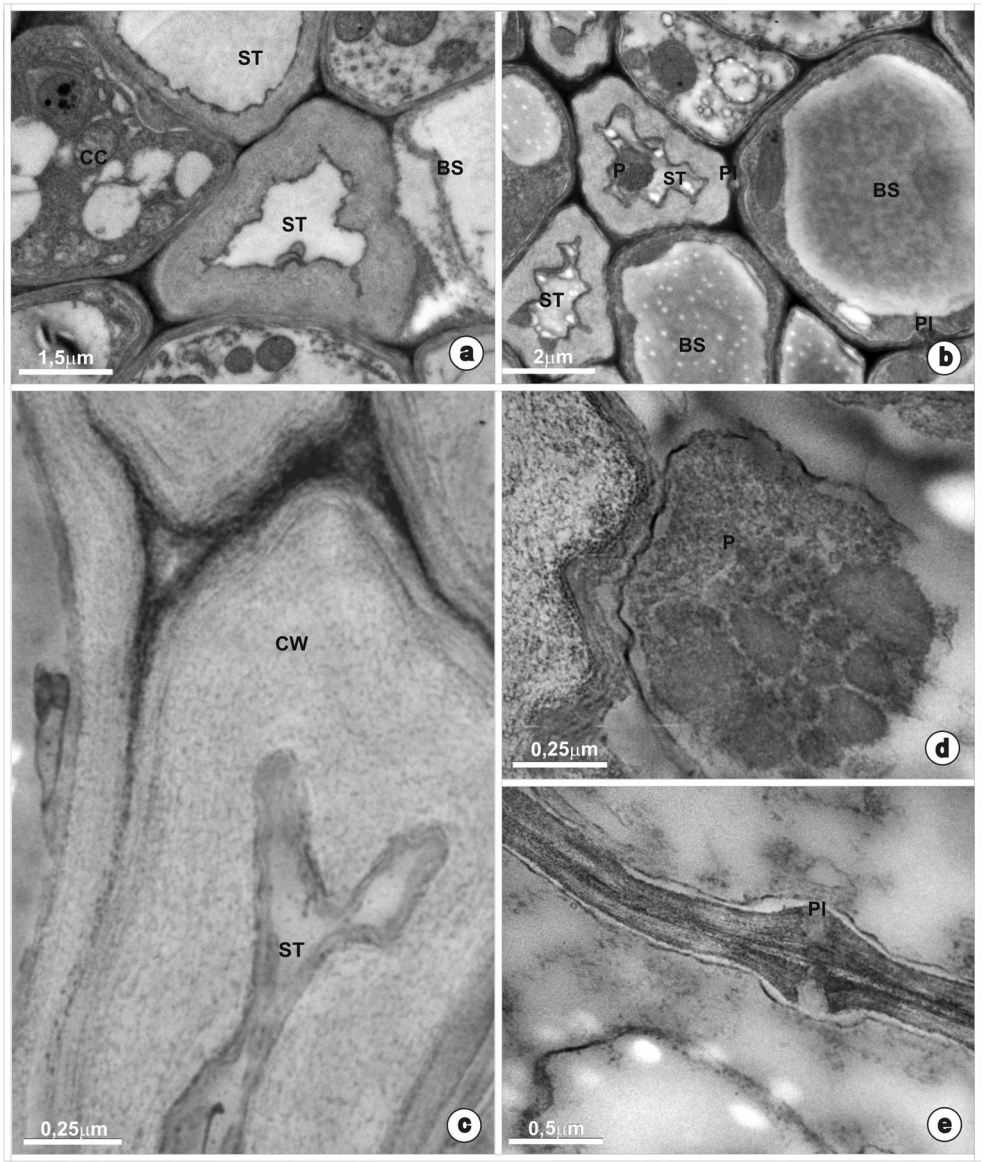


**Fig. 13** Transmission electron micrographs of transverse sections of the leaf blade midrib of *Halodule wrightii* Aschers. **a**, **b** Sieve tube elements with nacreous cell walls and plastids with protein inclusions. **c** Detail of the nacreous cell wall of the sieve tube element. **d** Detail of the P-type plastid with granular protein inclusions. **e** Details of a plasmodesma between two chlorenchyma cells. *BS* bundle sheath, *CC* companion cell, *CW* cell wall, *P* plastid with protein inclusion, *Pl* plasmodesma, *ST* sieve tube

cells and between sieve tube elements with chlorenchyma cells (Fig. 13b, e).

*Ruppia maritima*

Transmission electron micrographs of transverse sections of the leaf blade of *R. maritima* revealed epidermal cells with large amounts of chloroplasts distributed throughout the cytoplasm, with higher concentration in the peripheral region, a central small vacuole (Fig. 14a), and many mitochondria next to chloroplasts and anticlinal cell walls (Fig. 14b). Many expansions are visible in the cell walls of the epidermal cells (Fig. 14b, c, arrows). These expansions are found in anticlinal cell walls, and they sometimes also affect the external and internal periclinal walls. These expansions were not found in the mesophyll cells.

The outer periclinal cell wall of the epidermis cell is very thick compared to the inner periclinal wall (Fig. 14a, d), and four distinct zones can be observed: a thickened, nonelectron-dense layer can be seen from the inside to the outside, followed by another thickened, but electron-dense, layer, which appears to correspond to protein deposition observed under light microscopy (Fig. 8f, g), a third thin layer, even more electron-dense, and, finally, an externally located electron-transparent layer with the presence of small cavities (Fig. 14d, e, white arrows).

Idioblasts occur in the epidermis of *R. maritima*, but they were not observed under light microscopy. The idioblasts have many mitochondria located in the peripheral region of the cytoplasm, next to the mesophyll cells, as well as many vesicles and cell wall expansions, mainly the outer periclinal wall, occupying a large part of the cytoplasm (Fig. 14f). The

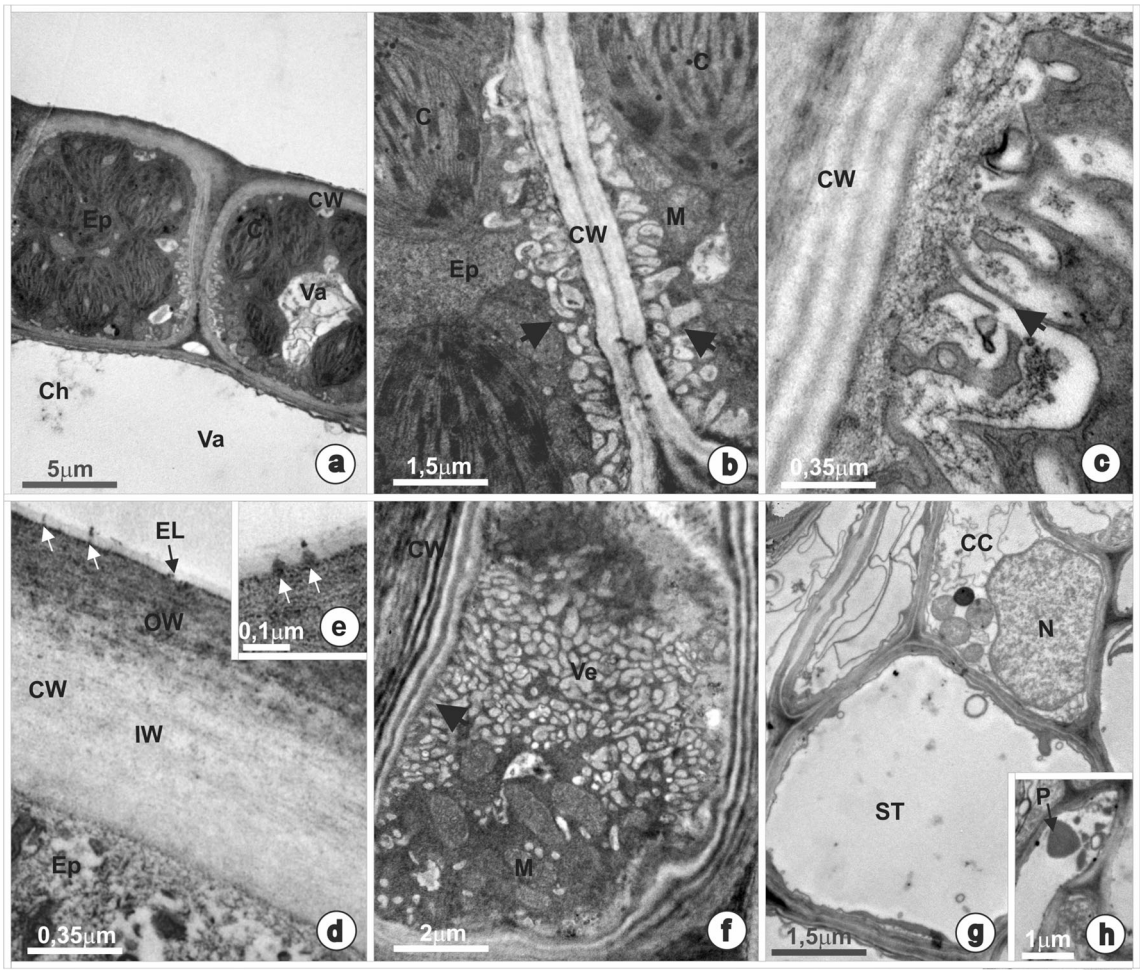


**Fig. 14** Transmission electron micrographs of transverse sections of the leaf blade of *Ruppia maritima* L. **a** Epidermal cells with the presence of a large amount of chloroplasts scattered throughout the cytoplasm, small vacuoles, and outer periclinal cell walls thicker than the inner; chlorenchyma cell with large central vacuole. **b** Detail of the epidermal cell showing the cell wall expansions (*arrows*) and mitochondria near the chloroplasts and expansions. **c** Highlight of the cell wall expansions (*arrow*). **d** Detail showing the outer periclinal cell walls with four distinct zones: a thickened, nonelectron-dense layer (*IW*) can be seen from the inside to the outside, followed by another thickened, but electron-dense layer (*OW*), a third thin layer (*black arrow*), even more electron-dense, and, finally, an electron-transparent layer with the presence of small cavities (*white arrows*). **e** Detail of the cavities (*white arrows*) of the electron-transparent layer of the epidermal cell wall. **f** Detail of an epidermal idioblast revealing the absence of chloroplasts and presence of large numbers of mitochondria, vesicles, and cell wall expansions. **g** Midrib showing companion cell and sieve tube element with thin walls. **h** Detail of the P-type plastid with cuneiform protein inclusions. *C* chloroplast, *CC* companion cell, *Ch* chlorenchyma, *Cu* cuticle, *CW* cell wall, *EL* electron-transparent layer, *Ep* epidermis, *IW* inner wall region, *M* mitochondria, *N* nucleus, *OW* outer wall region, *P* plastid with protein inclusion, *ST* sieve tube, *T* thylakoid, *Va* vacuole, *Ve* vesicles

external periclinal walls of these cells are also thicker, and chloroplasts were not found.

The mesophyll cells have thin walls and the presence of centrally located large vacuoles restricted to the periphery of the cytoplasm where chloroplasts and other organelles are distributed (Fig. 14a). In the central vascular bundle, companion cells and sieve tube elements are observed. Sieve tube elements have thin cell walls and large cell lumen (Fig. 14g). Inside of the sieve tube elements are found mitochondria and P-type plastids with cuneiform protein inclusions (Fig. 14h).

Chloroplasts of both epidermal (Fig.15a, b) and mesophyll cells (Fig. 15c, d) have an elliptical shape, with organized thylakoids and abundant plastoglobules, but with various particularities. The chloroplasts of the epidermis are increased in number, have higher amounts of thylakoids by granum and higher numbers of granum. Some mesophyll chloroplasts have starch grains, which are absent in the chloroplasts of the epidermis.

## Discussion

The main differences in the anatomical structure of seagrasses in relation to land plants include the absence of stomata, extremely thin cuticle, epidermis acting as the main photosynthetic site,

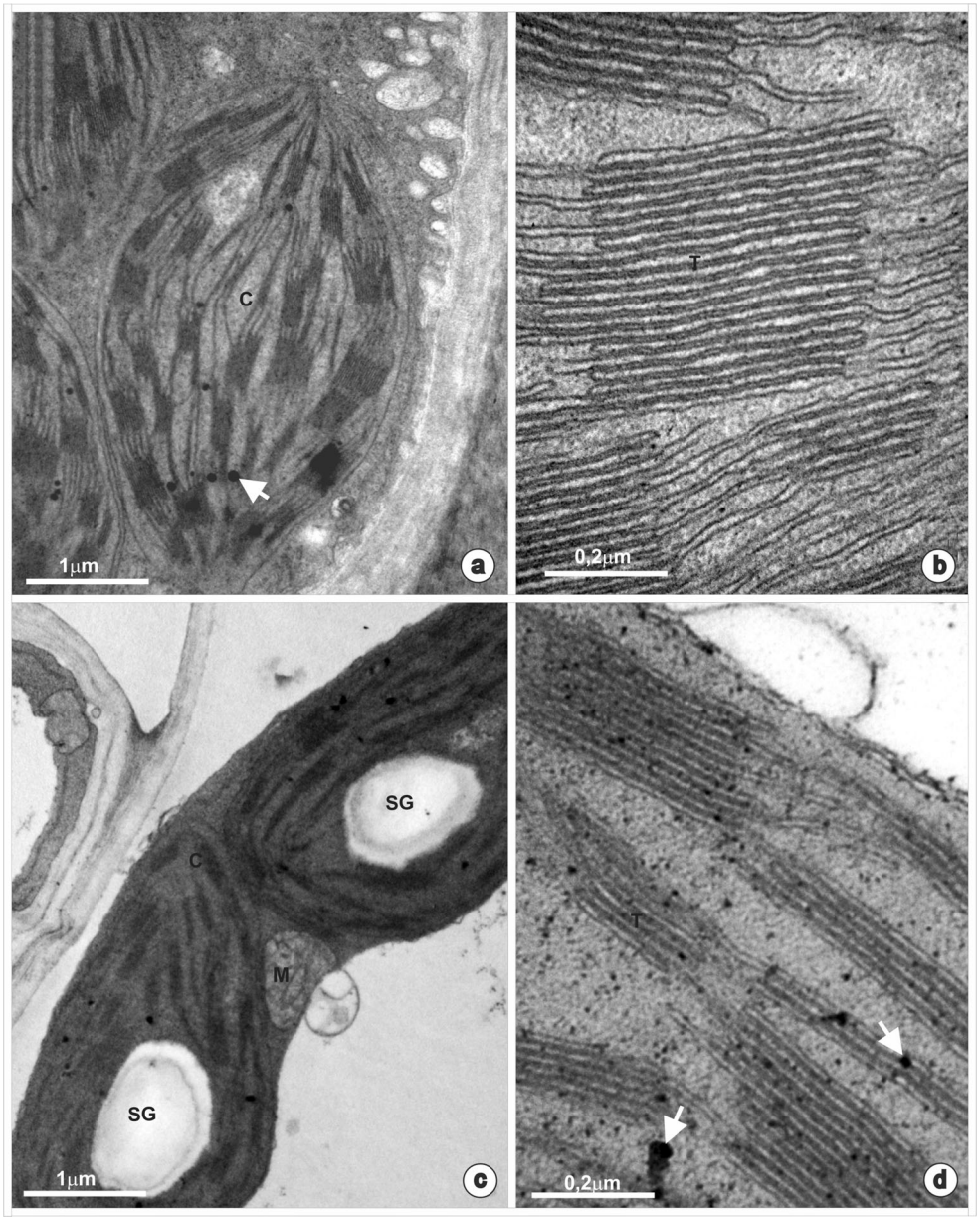


**Fig. 15** Transmission electron micrographs of transverse sections of the leaf blade of *Ruppia maritima* L., evidencing the chloroplasts of the epidermis (**a**, **b**) and mesophyll (**c**, **d**). **a**, **b** Detail of the structure of an epidermal chloroplast with organized thylakoid and presence of small plastoglobules (*white arrow*). **c** Chloroplast of the mesophyll cells with presence of starch grains. **d** Detail of the structure of a chlorenchymatic chloroplast with organized thylakoid and presence of small plastoglobules (*white arrow*). *C* chloroplast, *M* mitochondria, *SG* starch grain, *T* thylakoid

large intercellular spaces with vast system of aerenchyma, and reduced xylem, sometimes accompanied by a reduction in mechanical tissues (Kuo and den Hartog 2006). All these features were found in the three species studied in this work; however, some unique features were detected.

In the leaf blade of *H. wrightii* and *R. maritima*, we observed the presence of idioblasts containing phenolic contents. In plants, the group of phenolic contents includes simple phenols, phenolic acids, flavonoids, tannins, and lignins (Taiz and Zeiger 2009). These substances, which attract pollinators (Brouillard and Dangles, 1994), are generally associated with protection against herbivores and pathogens (Taylor and Grotewold 2005). Moreover, they protect against ultraviolet radiation (Carletti et al. 2003) and provide mechanical support (Castro and Machado 2006). However, many studies have also reported on the phenolic antioxidant function (Mendes 2009; Souza et al. 2009). According to Taiz and Zeiger (2009), salinity induces osmotic and ionic stress in plant cells, which, in turn, leads to oxidative stress, causing one of the primary effects of the greater accumulation of reactive oxygen species (ROS), which can result in severe damage to plants (Zhu 2001; Esteves and Suzuki 2008). To defend against these ROS, plants possess both enzymatic and nonenzymatic antioxidant systems (Pang and Wang 2008). The enzymatic system is characterized by its peroxidase content (Taiz and Zeiger 2009). The nonenzymatic system is characterized by presence of molecules such as ascorbic acid (vitamin C), tocopherol, and glutathione and phenolic contents, which together play an important role in the neutralization or sequestration of free radicals (Mendes 2009).

In addition to antioxidants, to prevent the harmful effects of salt stress, plants may develop other complex mechanisms that contribute to the adaptation to osmotic and ionic stresses; compartmentalization of ions in vacuoles is among these (Hogarth 2007; Esteves and Suzuki 2008; Souza et al. 2009). The present study verified that the content of idioblasts in both *H. wrightii* and *R. maritima* is stored in the vacuole and that such idioblasts move toward the epidermis where they break the outer periclinal cell walls, releasing the contents to the outside. This process corroborates the findings by Dickison (2000), who studied the leaves of many species of aquatic plants, which have secretory cells or tissues for salt accumulation in their interior. Such cells were found to be specialized in the accumulation and storage of these ions, which are subsequently expelled to the outside surface of the leaf. In *H. wrightii* and *R. maritima*, this seems to be one of the strategies of adaptation to salinity, i.e., excess salt accumulated in specialized cells, using the resource of the phenolic contents to prevent damage from ROS, forming an environmental stockpile that will soon be eliminated. In *H. wrightii*, these idioblasts were found in the epidermis and in the mesophyll near the epidermis; these ions are taken up by the epidermal cells of the leaf blade and subsequently deposited in the subepidermal layer of the mesophyll. In *R. maritima*, the idioblasts were seen in all tissues of the leaf, including the midrib. It appears that this species is also capable of transferring excess salts absorbed by the roots to the epidermal layer from which they are, in turn, expelled. More detailed studies on the idioblasts of these species should be conducted to clarify their pathways and adaptive strategies.

Another type of idioblast is found in both *H. wrightii* and *R. maritima*, which can only be observed under TEM. They are differentiated from epidermal cells by the thick outer periclinal cell wall, a lack of chloroplasts, the large cluster of mitochondria located in the peripheral region of the cytoplasm near the mesophyll, and the numerous vesicles and cell wall projections that occupy much of the cytoplasm. Expansions of the epidermal cell wall were observed in *Thalassia testudinum* by Jagel (1973). The author suggested that these expansions could be associated with osmoregulation, similar to that found in the secretory cells of mangrove plants. By studying the salt glands of *Tamarix aphylla* L., Bosabalidis (2010) realized that such structures possess several projections of the cell wall and that the number of mitochondria and microvacuoles increases in its vicinity. According to Pang and Wang (2008), mitochondria are specialized organelles used to combat ROS because they possess both enzymatic and nonenzymatic antioxidant systems, as described above. According to Metcalfe and Chalk (1979), in specialized cells of aquatic plants, called hydropoten, numerous vesicles, mitochondria, and many projections of the cell wall are present in the cytoplasm. The species *H. decipiens* has trichomes throughout the leaf margin. According to Alquini et al. (2006), trichomes usually found on the surfaces of submerged leaves of aquatic plants may be involved in the transport of water and salts; these structures are given the special name of hydropoten. Fahn (1979) describes how these trichomes play an important role in the transport of water and salts into and out of aquatic plants, absorbing two to three times more than the other cells of the epidermis. Such structural peculiarities suggest that hydropoten actively works in the transport of minerals. Therefore, the three species have hydropotens; in *H. wrightii* and *R. maritima*, the hydropotens are similar to other common epidermal cells, but with distinct ultrastructural characteristics, and in *H. decipiens*, the hydropotens are trichomes that occur in the leaf margins.

The presence of trichomes on the leaf surface in the specimens of *H. decipiens* from São Paulo may also be related to water quality, increasing with the increase of water pollution, since the specimens were collected from Bahia in the Abrolhos Archipelago, which is a marine national park and is in a conservation unit. Specimens of São Paulo, in turn, were collected on the beach from Saco da Ribeira (Ubatuba), where there is a large concentration of businesses aimed at tourism and boating activity as a result of the installation of piers and wharves. According to the report entitled "Quality of Surface Water in the State of São Paulo-2010" (CETESB 2011), samples collected at the Saco da Ribeira reveal sediment with negative redox potential, indicating environmental anaerobic decomposition of organic material. In addition, considering all points of the Coastal Network from São Paulo, higher levels of total phosphorus were obtained in this region. Souza et al. (2009) also noted an increase in the number of trichomes in two species of aquatic macrophytes subjected to high concentrations of the metal cadmium (Cd), which is a chemical used in industry and many base pigments, including those used in nautical vessels.

These cell wall expansions were also visualized, albeit in small numbers, in other epidermal cells of the leaf blade, including in epidermal cells of *H. decipiens*. These wall expansions are always accompanied by mitochondria, and occur mainly in anticlinal cell walls, but in smaller quantities in the outer and inner periclinal walls. Such expansions were not found in the mesophyll cells, even those in direct contact with the epidermis. Kuo and den Hartog (2006) also viewed these expansions in the epidermis of the leaf blades of seagrasses they analyzed, terming them as "wall ingrowths". Doohan and Newcomb (1976), studying the anatomy of *Cymodocea rotundata* Ehrenb. and Hempr., *Cymodocea serrulata* (R. Br) Aschers. and Magnus, and *Thalassia hemprichii* (Ehrenb.) Aschers, also found these epidermal cell wall expansions, which indicated extensive similarity to transfer cells, suggesting that these cells were involved in short-distance transport and absorption of solutes from the surrounding water. Kuo (1978) studied the anatomy of

*Posidonia australis* Hook F. and found that this species of seagrass did not have these "wall ingrowths." However, the author reported that *P. australis* had polyphenolic substances able to control salt stress. Besides adapting to a saline environment, these expansions of the cell wall enable the seagrass species to perform transport of water and nutrients through the leaves, explaining the reduction of vascular elements, especially xylem elements, which were not observed in species in which only protoxylem lacunae occur.

Proteins in all species analyzed in this study show up in the outer portion of the periclinal cell wall of epidermal cells, as also noted by Kuo and den Hartog (2006), a previously cited anatomical study of seagrasses, which also reported the presence of polysaccharides, low cellulose, and absence of lignin. According to Zhu (2001), the accumulation of nitrogenous compounds in plants is related to salt tolerance, acting as a form of osmotic adjustment, as well as protecting cellular macromolecules, storing nutrients, maintaining cellular pH, detoxifying cells, and minimizing the effects of ROS (Esteves and Suzuki 2008). *H. wrightii* and *R. maritima* also had concentrations of polysaccharides and proteins in the cytoplasm of the epidermis, and *H. decipiens* showed these concentrations in the outer region of the cytoplasm of the trichomes. Under conditions of salt stress, plants accumulate various osmolytes, such as organic solutes, including sugars, amino acids, and proteins, which can concentrate in distinctly different plant parts, presenting different physiological effects. Some may be enzymes and protect structures, while others may contribute to the osmotic balance of the plant (Garcia et al. 1997; Marcondes and Garcia 2009).

Another adaptation to the marine environment, as observed in the present seagrass study, was the occurrence of a thin cuticle. In the specimens of *H. wrightii* and *R. maritima*, this thin cuticle has small subcuticular cavities, which were also observed by Kuo and den Hartog (2006) in some species of seagrasses. Kuo (1978) recorded the presence of pores with a thin cuticle on the leaf blades from the seagrass *P. australis* Hook F., and according to the author, these pores are used to increase the flow of nutrients and water exchange between the seagrass and the surrounding water, as well as facilitate gas exchange (Hemminga and Duarte 2000). According to Mauseth (2009), the cuticle is a layer consisting of cutin located after the pectic layer, which adheres to the wall of epidermal cells. Besides the cuticular layer, the authors suggest that the epidermal cells may have a layer consisting of epicuticular waxes external to the cuticular layer and also cuticular extracts in the outer periclinal walls of epidermal cells, especially in the more outer portion. Lyshede (1980) divides the cuticle into five layers, from the most external region to the most internal, as follows: (1) epicuticular layer formed by waxes; (2) cuticle itself formed only by cutin; (3) cutinized layer formed by cutin, cellulose, pectin, and waxes; (4) pectic layer formed exclusively of pectin, which forms the limit of the outer periclinal cell wall of the epidermis; and (5) cellulosic layer, consisting of cellulose and pectin, the latter layer being the outer portion of the outer periclinal walls of the epidermis.

According to Lyshede (1980), the transmission electron micrographs of the leaf of *H. wrightii* and *R. maritima* revealed a cuticle with three layers: layer 5, cellulosic, which is shown in more electron-dense micrographs; layer 4, pectin, more electron-dense; and a third layer, which proved to be electron-transparent, showing, in these two species, the presence of small subcuticular cavities. However, it was not possible to identify the composition. It is likely that the addition of pectin will also occur in the presence of protein in layer 5, since there was a positive reaction to CBB in this region. Also, it has been reported that seagrasses make the enzymatic conversion of bicarbonate ions ($HCO_3^-$) in seawater to $CO_2$, mediated by enzymatic activity that occurs in the outer periclinal walls of the epidermal cells (den Hartog and Kuo 2006). Zhu (2001) also reports, as previously mentioned, that the accumulation of nitrogenous compounds in plants is also related to tolerance to salinity. In *H. decipiens*, the cuticle is formed by only two layers: cellulose (5) and pectin (4). Generally speaking, the three species analyzed have a thin cuticle, a common characteristic for submerged macrophyte leaves, enabling improved nutrient uptake by epidermal cells (Menezes et al. 2006). Compared with the other species analyzed, *H. decipiens* has the thinnest cuticle; this feature may be related to the great depths and low radiation where this plant can be found, up to 62 m (Oliveira Filho et al. 1983), since according to Dickison (2000), increasing the number of layers and their thickness can prevent the excessive irradiation inside the plant. Besides the reduction of the cuticular layer, *H. decipiens* shows other morphological adaptations to the low light environment, including a thin cell wall and chloroplasts located in the outer periphery of the epidermal cell.

Another adaptive feature present in aquatic species is the presence of aerenchyma that constitutes real networks interconnecting all organs. This tissue was also observed in the leaves of species from the present study. In *H. decipiens* and *R. maritima*, the air lacunae are constant, always two lacunae, with one on each side of the midrib. In *R. maritima*, the diameter is larger. In *H. wrightii*, the number of air lacunae in the leaf blade is not constant, increasing with the expansion of the width and thickness of the leaf blade. These lacunae can store the carbon dioxide produced by respiration of leaves for photosynthesis and certainly carry oxygen to the roots for respiration (Hemminga and Duarte 2000). Often, the sediment occupied by seagrasses is low in oxygen, and without this means of gas transportation, the submerged life for these aquatic plants would be impossible (Duarte 2002). The oxygen that is released by roots also positively affects the survival and growth of other organisms (Hogarth 2007), including fungal and bacterial endophytes, which through the work of

Shoemaker and Wyllie-Echeverria (2013) have been isolated from the rhizomes of three species of seagrasses. The study of $O_2$ transport in plants conducted by Sand-Jensen et al. (2005) showed that the intra-plant transport of $O_2$ and other gases between leaf and root tips takes place more readily in plants that have shorter distances and greater cross sections of uninterrupted gas-filled lacunae. Within the leaves, the air lacunae also confer buoyancy, helping to raise the photosynthetic apparatus and maximize capture of light (Hemminga and Duarte 2000).

This anatomical data reinforces that the major morphoanatomical adaptations to the marine environment are observed in all analyzed species (*H. decipiens*, *H. wrightii*, *and R. maritima*) independent of their evolutionary affinities (Les and Tippery 2013). Therefore, the presence of idioblasts, containing phenolic compounds, is important in the neutralization or sequestration of free radicals caused by salt stress in *H. wrightii* and *R. maritima*. In the same direction, presence of hydropotens and cell wall expansions in epidermal cells, in all evaluated species, represent a single adaptive tool for changes in salinity. The reduction of vascular elements, thin cuticle, and air lacunae represent answers to the subtidal life evolutionarily imposed on these groups, which came originally from land environments.

**Acknowledgments** We are grateful for the staff of the Laboratory of Plant Anatomy (LAVEG/UFSC), Laboratory of Marine Algae (LAMAR/UFSC), Laboratory Studies in Biology Multiuser II (LAMEB II/UFSC), and for the Central Laboratory of Electron Microscopy (LCME/UFSC) for all the help provided and for making space and equipment available in these laboratories and to Conselho Nacional de Pesquisa (CNPq) for granting the fellowship for the second author. This study is part of the master's degree of the first author.

**Conflict of interest** The authors declare that they have no conflict of interest.

## References

Alquini Y, Bona C, Boeger MRT, Costa CG, Barros CF (2006) Epiderme. In: Appezzato-da-Gloria B, Carmello-Guerreiro SM (eds) Anatomia vegetal, 2nd edn. UFV, Viçosa, pp 87–97

Bosabalidis AM (2010) Wall protuberance formation and function in secreting salt glands of *Tamarix aphylla* L. Acta Bot Bras 69:229–235

Brouillard R, Dangles O (1994) Flavonoids and flower colour. In: Harborne JB (ed) The flavonoids: advances in research since 1986. Chapman and Hall, London, pp 565–588

Carletti P, Masi A, Wonisch A, Grill D, Tausz M, Ferretti M (2003) Changes in antioxidant and pigment pool dimensions in UV-B irradiated maize seedlings. Environ Exp Bot 50:149–157

Castro MM, Machado SR (2006) Células e tecidos secretores. In: Appezzato-da-Gloria B, Carmello-Guerreiro SM (eds) Anatomia Vegetal, 2nd edn. UFV, Viçosa, pp 179–203

Copertino MS (2011) Add coastal vegetation to the climate critical list. Nature 473:255

Creed JC, Paixão AM, Aoki AL, Barbosa MBS, Moreira D, Patrício ED, Casares FA, Almeida M (2004) Monitoramento de fanerógamas marinhas no arquipélago dos Abrolhos-BA. In: Programa SeagrassNet: Relatório de Atividades entre abril 2003 a agosto 2004. Ministério do Meio Ambiente, Brasília, Brasil

CETESB Companhia de Tecnologia de Saneamento Ambiental (2011) Qualidade das águas Superficiais no Estado de São Paulo 2010. Recurso eletrônico CETESB. http://www.cetesb.sp.gov.br/agua/aguas-superficiais/35-publicacoes-/-relatorios. Accessed 15 July 2012

den Hartog C (1970) The sea-grasses of the world. North-Holland Publishing Company, Amsterdam

den Hartog C, Kuo J (2006) Taxonomy and biogeography of seagrasses. In: Larkum AWD, Orth RJ, Duarte CM (eds) Seagrasses: biology, ecology and conservation. Springer, The Netherlands, pp 1–29

Dickison WC (2000) Integrative plant anatomy. Harcourt/Academic Press, Massachusetts

Doohan ME, Newcomb EH (1976) Leaf ultrastructure and δ13C values of three seagrasses from the great barrier reef. Aust J Plant Physiol 3: 9–23

Duarte CM (2002) The future of seagrass meadows. Environ Conserv 29: 192–206

Esteves BS, Suzuki MS (2008) Efeito da salinidade sobre as plantas. Oecol Bras 12:662–679

Fahn A (1979) Secretory tissues in plants. Academic, New York

Fonseca MS, Fisher JS (1986) A comparison of canopy friction and sediment movement between 4 species of seagrass with reference to their ecology and restoration. Mar Ecol-Prog Ser 29:15–22

Gahan PB (1984) Plant histochemistry and cytochemistry: an introduction. Academic, London

Garcia AB, Engler JA, Iyer S, Gerats T, Van Montagu M, Caplan AB (1997) Effects of osmoprotectants upon NaCl stress in rice. Plant Physiol 115:159–169

Gordon EM, McCandless EL (1973) Ultrastructure and histochemistry of *Chondrus crispus* Stack. P N S I Sci 27:111–133

Gullström M, de la Torre Castro M, Bandeira S, Björk M, Dahlberg M, Kautsky N, Rönnbäck P, Öhman MC (2002) Seagrass ecosystems in the Western Indian ocean. AMBIO J Human Environ 31:588–596

Hemminga M, Duarte CM (2000) Seagrass ecology. Cambridge University Press, Cambridge

Hogarth PJ (2007) The biology of mangroves and seagrasses. Oxford University Press, New York

Jagel RH (1973) Studies of a marine grass *Thalassia testudinum*. I. Ultrastructure of osmoregulatory leafcefts. Am J Bot 60:1003–1009

Johansen DA (1940) Plant microtechnique. McGraw Hill Book Company, New York

Kuo J (1978) Morphology, anatomy and histochemistry of the Australian seagrasses of the genus *Posidonia* könig (posidoniaceae). I. Leaf blade and leaf sheath of *Posidonia australis* hook *F.* Aquat Bot 5: 171–190

Kuo J, den Hartog C (2006) Seagrass morphology, anatomy, and ultrastructure. In: Larkum AWD, Orth RJ, Duarte CM (eds) Seagrasses: biology, ecology and conservation. Springer, The Netherlands, pp 51–87

Larkum WD, Orth RJ, Duarte CM (2006) Seagrasses: biology, ecology and conservation. Springer, The Netherlands, 691p

Les DH, Tippery NP (2013) In time and with water…the systematics of alismatid monocotyledons. In: Wilkin P (ed) Early events in monocot evolution. Cambridge University Press, Cambridge, pp 118–164

Les DH, Cleland MA, Waycott M (1997) Phylogenetic studies in the monocot subclass Alismatidae II: evolution of marine angiosperms ("seagrasses") and hydrophily. Syst Bot 22:443–463

Lyshede OB (1980) Structure of the outer epidermal wall in xerophytes. In: Cutler DF, Alvin KF, Price CE (eds) The plant cuticle. Academic, London, pp 87–98

Marcondes J, Garcia AB (2009) Aspectos citomorfologicos do estresse salino em plântulas de arroz (*Oryza sativa* L.). Arq Inst Biol 76:187–194

Mauseth JD (2009) Botany: an introduction to plant biology, 4th edn. Jones and Bartlett Publishers, Boston

McCoy ED, Heck KL (1976) Biogeography of corals, seagrasses and mangroves: an alternative to the centre of origin concept. Syst Zool 25:201–210

Mendes BSS (2009) Efeitos fisiológicos e bioquímicos do estresse salino em *Ananas porteanus* Hort Veitch ex C. Koch. Dissertation, Federal Rural University of Pernambuco

Menezes NL, Silva DC, Pinna GFM (2006) Folha. In: Appezzato-da-Gloria B, Carmello-Guerreiro SM (eds) Anatomia vegetal, 2nd edn. UFV, Viçosa, pp 87–97

Metcalfe CR, Chalk L (1979) Anatomy of the dicotyledons, vol 1, 2nd edn. Claredon Press, Oxford

Oliveira Filho EC, Pirani JR, Giulietti AM (1983) The Brazilian seagrass. Aquat Bot 16:251–267

Oliveira EC, Horta PA, Amâncio CE, Sant'anna CL (1999) Algas e angiospermas marinhas bênticas do litoral brasileiro: diversidade, exploração e conservação. In: Workshop sobre avaliação e ações prioritárias para conservação da biodiversidade das zonas costeira e marinha. Relatório Técnico. Ministério do Meio Ambiente, Brasília, Brasil, 2002. 1 CD-ROM

Orth RJ, Carruthers TJB, Short FT, Dennison WC, Duarte CM, Fourqurean JW, Heck KL, Hughes AR, Kendrick GA, Kenworthy WJ, Olyarnik S, Waycott M, Williams SL (2006) A global crisis for seagrass ecosystems. Bio Sci 56:987–996

Pang CA, Wang B (2008) Oxidative stress and salt tolerance in plants. Prog Bot 69:231–246

Sand-Jensen K, Pedersen O, Binzer T, Borum J (2005) Contrasting oxygen dynamics in the freshwater isoetid Lobelia dortmanna and the marine seagrass Zostera marina. Ann Bot 96:613–623

Shoemaker G, Wyllie-Echeverria S (2013) Occurrence of rhizomal endophytes in three temperate northeast pacific seagrasses. Aquat Bot 111:71–73

Short FT, Neckles HA (1999) The effects of global climate change on seagrasses. Aquat Bot 63:169–196

Short FT, Koch EW, Creed JC, Magalhães KM, Fernandez E, Gaeckle JL (2006) SeagrassNet monitoring across the Americas: case studies of seagrass decline. Mar Ecol 27:277–289

Souza VL, Silva DC, Santana KB, Mielke MS, Almeida AF, Mangabeira PA, Rocha EA (2009) Efeito do cádmio na anatomia e na fotossíntese de duas macrófitas aquáticas. Acta Bot Bras 23:343–354

Taiz L, Zeiger E (2009) Fisiologia vegetal, 4th edn. Artmed, Porto Alegre

Taylor LP, Grotewold E (2005) Flavonoids as developmental regulators. Curr Opin Plant Biol 8:317–323

Waycott M (2000) Mating systems and population genetics of marine angiosperms (seagrasses). In: Wilson KL, Morrison D (eds) Monocots: systematics and evolution, vol 1. CSIRO Publishing, Sydney, pp 277–285

Zhu JK (2001) Plant salt tolerance. Trends Plant Sci 6:66–71